

## Effect of heat treatment conditions on microstructure and magnetic property of $\text{Fe}_{77}\text{Co}_2\text{Zr}_9\text{B}_{10}\text{Cu}_2$ alloy

W. Q. Yu\*, X. C. Meng\*, B. Zuo\*, Y. M. Sun\*, B. Li<sup>†</sup> and Z. Hua\*,<sup>‡</sup>

\*Key Laboratory of Functional Materials Physics and Chemistry of the Ministry of Education, Jilin Normal University, Siping 136000, Jilin, China

<sup>†</sup>Changchun Institute of Optics, Fine Mechanics and Physics, Chinese Academy of Sciences, Dong Nanhu Road 3888, Changchun 130012, China

<sup>‡</sup>huazhong196110@163.com

Received 5 November 2013

Revised 31 March 2014

Accepted 1 April 2014

Published 6 May 2014

$\text{Fe}_{77}\text{Co}_2\text{Zr}_9\text{B}_{10}\text{Cu}_2$  alloy prepared by melt-spinning was annealed at different heat treatment conditions. The thermal property, microstructure and magnetic property of alloys were investigated by differential thermal analysis (DTA), X-ray diffraction (XRD), transmission electron microscopy (TEM) and vibrating sample magnetometer (VSM).  $\text{Fe}_{77}\text{Co}_2\text{Zr}_9\text{B}_{10}\text{Cu}_2$  alloy as-quenched is a mixture of  $\alpha$ -Fe(Co) phase, H-phase and amorphous phase. With increasing annealing temperature, the H-phase transforms to  $\alpha$ -Fe(Co) phase. Coercivity ( $H_c$ ) of  $\text{Fe}_{77}\text{Co}_2\text{Zr}_9\text{B}_{10}\text{Cu}_2$  alloy annealed at 600°C for 40 min followed by furnace cooling reaches the minimum value, which is attributed to the small and homogeneous  $\alpha$ -Fe(Co) grain structure.

**Keywords:** Microstructure; magnetic property.

### 1. Introduction

Over the past several decades, extensive researches have been carried out on FeZrB-based nanocrystalline alloys.<sup>1–8</sup> FeZrB amorphous alloy has been reported to exhibit excellent soft magnetic properties after being annealed under optimal conditions, when they reach a nanocrystalline (Nanoperm) microstructure characterized by a nanometric bcc-Fe phase surrounded by a residual amorphous matrix.<sup>2</sup> Both grain size ( $D$ ) and volume fraction of  $\alpha$ -Fe are the most important factors for controlling the soft magnetic properties. Suzuki *et al.*<sup>9,10</sup> have shown that the coercivity of Nanoperm type FeZrB(Cu) follows a simpler  $D^3$  power law.

The procedure of quenching and subsequent annealing is a basic approach to control the microstructure of materials and thereby to achieve the special properties for the final product. Numerous systematic studies on annealing condition such as temperature and period have been made to obtain a fine grain size of  $\alpha$ -Fe(Co).<sup>11–13</sup>

Table 1. The heat treatment parameters of the investigated alloy.

Annealing temperature (°C)	Heating rate (°C/min)	Holding time (min)	Cooling method
530	10	40	Furnace cooling
600	10	20	Furnace cooling
600	10	40	Furnace cooling
600	10	40	Liquid-nitrogen cooling
600	10	80	Furnace cooling
600	10	120	Furnace cooling
670	10	40	Furnace cooling
750	10	40	Furnace cooling

The initial crystallization product of Fe-based amorphous alloy is generally body-centered cubic (b.c.c.)  $\alpha$ -Fe phase (lattice constant  $a = 2.866$  nm). Moreover, Lyasotskii *et al.*<sup>14,15</sup> studied the Fe–Si–B–Nb alloys and observed a number of special crystallization phases. These phases reported are related to the  $\alpha$ -Mn structure type. The H-phase is reported as hexagonal phase (rhombohedral distortion of  $\alpha$ -Mn structure,  $a \sim 1.23$  nm,  $c \sim 0.77$  nm).<sup>15</sup>

In this work,  $\text{Fe}_{77}\text{Co}_2\text{Zr}_9\text{B}_{10}\text{Cu}_2$  alloys are prepared by melt-spinning and annealed at different heat treatment conditions. The H-phase is detected in the  $\text{Fe}_{77}\text{Co}_2\text{Zr}_9\text{B}_{10}\text{Cu}_2$  alloy as-quenched, which is little reported in other FeZrB-based alloys. The main aim of this paper is to study the effect of heat treatment conditions, i.e. temperature, holding time and cooling condition on microstructure and magnetic property of  $\text{Fe}_{77}\text{Co}_2\text{Zr}_9\text{B}_{10}\text{Cu}_2$  alloy.

## 2. Experimental Details

$\text{Fe}_{77}\text{Co}_2\text{Zr}_9\text{B}_{10}\text{Cu}_2$  ribbons about 7.5 mm in width and 35  $\mu\text{m}$  in thickness were prepared using single roller melt-spinning equipment with copper wheel rotating at a surface velocity of 30 m/s. The as-quenched ribbons were sealed in evacuated quartz tubes with the diameter of 8 mm and then annealed in the furnace. The heat treatment parameters were shown in Table 1.

The thermal property was investigated by differential thermal analysis (DTA, TG/DTA-6300). Microstructures were examined by X-ray diffraction (XRD, D/max 2500/PC, using radiation Cu-K $\alpha$ ,  $\lambda = 1.5406$  Å) and transmission electron microscopy (TEM, JEM-2100E, 200 kV). Grain size ( $D$ ) of  $\alpha$ -Fe(Co) was calculated by Scherrer formula  $D = 0.89\lambda/\beta \cos \theta$  ( $\beta$  indicates the width of half-height diffraction peak,  $\theta$  is Bragg angle,  $\lambda$  is X-ray wavelength, and  $D$  is grain size). Magnetic property was measured by vibrating sample magnetometer (VSM, Lake Shore M7407).

## 3. Results and Discussion

The XRD patterns from the free and contact surfaces of  $\text{Fe}_{77}\text{Co}_2\text{Zr}_9\text{B}_{10}\text{Cu}_2$  alloy as-quenched are shown in Fig. 1. The inset shows the corresponding DTA curve.

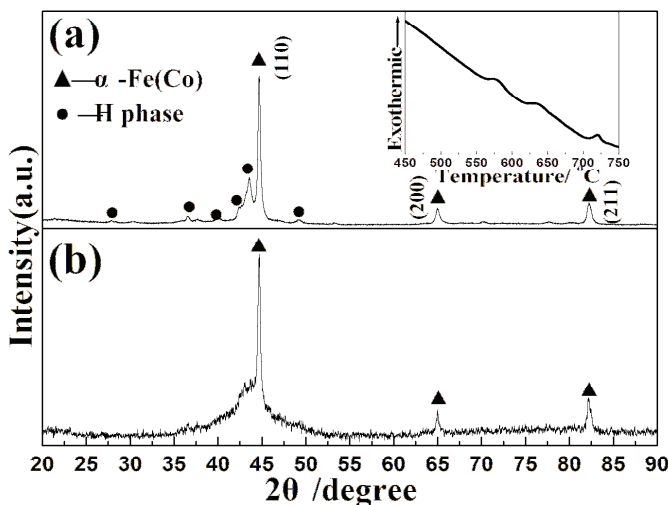


Fig. 1. XRD patterns from the free and contact surfaces of  $Fe_{77}Co_2Zr_9B_{10}Cu_2$  alloy as-quenched. The corresponding DTA curve is shown in the inset.

Table 2. The values of heats of mixing between Fe/Cu and other elements.

Heats of mixing (kJ/mol)				
	Fe	Co	Zr	B
Fe		-1	-25	-26
Cu	+13	+6	-23	0

Microstructures in the rapidly quenched (RQ) ribbons are usually inhomogeneous between free and contact surfaces of the ribbon. The H-phase,  $\alpha$ -Fe(Co) phase and amorphous phase were observed in RQ ribbon. The content of H-phase in the free surface is higher than that in the contact surface, and the corresponding amorphous phase in the free surface is lower than that in the contact surface. The lattice parameters of the H-phase calculated from free surface are  $a = 1.25$  nm and  $c = 0.78$  nm ( $c/a = 0.625$ ).  $Fe_{77}Co_2Zr_9B_{10}Cu_2$  alloy differs from the amorphous alloy previously studied by us mainly by substitution of iron by 2 at.% Cu.<sup>16</sup> This alloy has lower glass forming ability, which is partially crystalline. The values of heats of mixing between Fe/Cu and other elements<sup>17</sup> are shown in Table 2. The addition of 2 at.% Cu decreases the negative heats of mixing, which is bad for the amorphous formation ability.

According to the DTA curve, the alloy as-quenched is annealed at 530, 600, 670 and 750°C. The XRD patterns from the free (a) and contact (b) surfaces of  $Fe_{77}Co_2Zr_9B_{10}Cu_2$  alloys corresponding to different annealing temperatures followed by furnace cooling are shown in Fig. 2. XRD patterns between free and

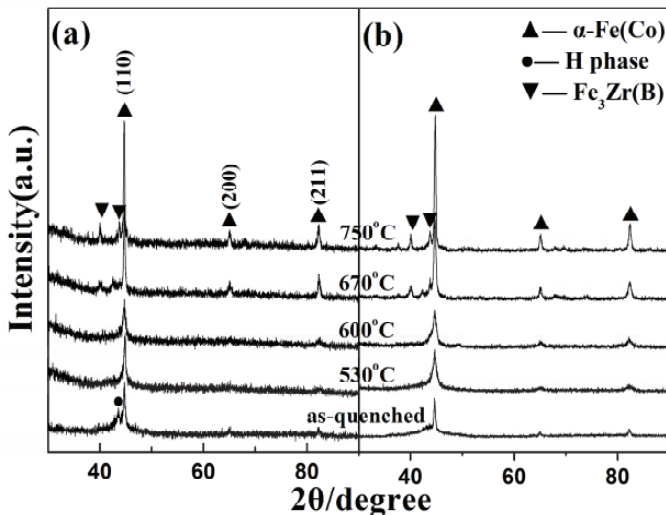


Fig. 2. XRD patterns from the free and contact surfaces of  $\text{Fe}_{77}\text{Co}_2\text{Zr}_9\text{B}_{10}\text{Cu}_2$  alloys corresponding to different annealing temperatures followed by furnace cooling.

contact surface after heat treatment have little difference. Further increase of annealing temperature leads to the disappearance of H-phase and the further crystallization of residual amorphous phase. The H-phase is metastable and transforms to  $\alpha$ -Fe(Co) phase during thermal crystallization. After annealing above 67°C,  $\text{Fe}_3\text{Zr}(\text{B})$  phase precipitates. Huang *et al.* indicated that the B atoms prefer to stay in the lattice of the  $\text{Fe}_3\text{Zr}$  phase.<sup>18</sup> The three exothermal peaks in the DTA curve correspond to the transformation of H-phase, the crystallization of residual amorphous phase and the precipitations of  $\text{Fe}_3\text{Zr}$  intermetallic compounds, respectively. According to Figs. 1 and 2, the microstructures of free surface are more representative. Moreover, microstructures are all taken from the free surface in the following text.

Figure 3 shows the TEM images of  $\text{Fe}_{77}\text{Co}_2\text{Zr}_9\text{B}_{10}\text{Cu}_2$  alloy as-quenched (a) and annealed at 600°C (b) followed by furnace cooling. The distribution of grain size is non-uniform and some amorphous phase is observed in Fig. 3(a). Figure 3(b) shows that the degree of crystallinity increases obviously and the grains are smaller and homogeneous.

Figure 4 shows the coercivity ( $H_c$ ) as a function of annealing temperature ( $T_a$ ). After annealing at 600°C,  $H_c$  reach the minimum value, which is mainly related to the small and homogeneous grains. Above 670°C, the rapid increase of  $H_c$  is mainly ascribed to the precipitations of  $\text{Fe}_3\text{Zr}(\text{B})$ .

The XRD patterns of  $\text{Fe}_{77}\text{Co}_2\text{Zr}_9\text{B}_{10}\text{Cu}_2$  alloys annealed at 600°C for 20, 40, 80 and 120 min are shown in Fig. 5. After annealing at 600°C for 40 min, the diffraction peaks of  $\alpha$ -Fe(Co) broaden, which is related to the refinement of grains. After annealing at 600°C for 80 min and 120 min,  $\text{Fe}_3\text{Zr}(\text{B})$  phase precipitates.

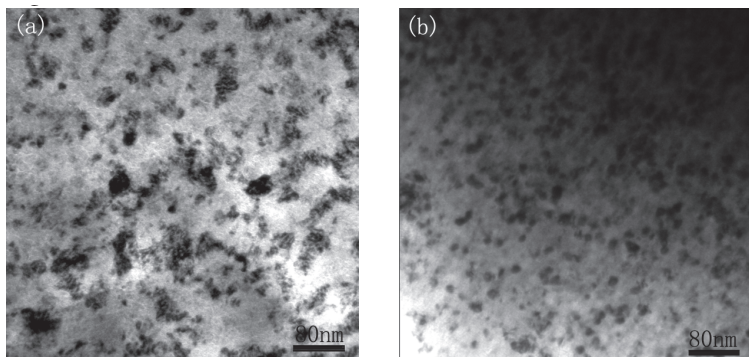


Fig. 3. Bright-field (BF) TEM of  $Fe_{77}Co_2Zr_9B_{10}Cu_2$  alloy as-quenched (a) and annealed at 600°C and (b) followed by furnace cooling.

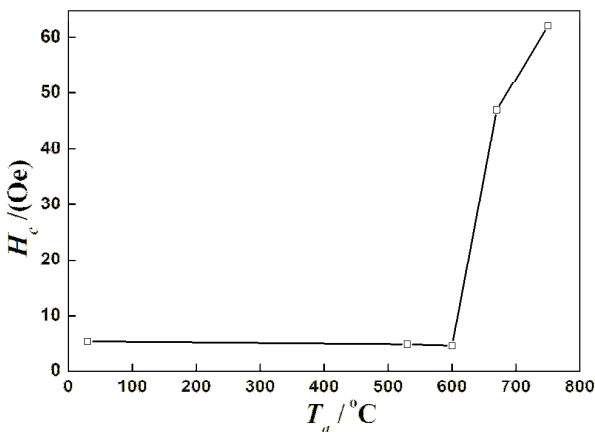


Fig. 4. Coercivity ( $H_c$ ) of  $Fe_{77}Co_2Zr_9B_{10}Cu_2$  alloy as a function of annealing temperature ( $T_a$ ).

The grain size ( $D$ ) of  $\alpha$ -Fe(Co) and coercivity ( $H_c$ ) as a function of holding time are shown in Fig. 6. Both the grain size ( $D$ ) of  $\alpha$ -Fe(Co) and coercivity ( $H_c$ ) of  $Fe_{77}Co_2Zr_9B_{10}Cu_2$  alloy annealed at 600°C for 40 min reach the minimum value and then increase. The grain size depends on the ratio between the nucleation rate and the crystal growth rate.<sup>19</sup> In this paper, H-phase transforms to  $\alpha$ -Fe(Co) phase and the amorphous phase crystallizes into  $\alpha$ -Fe(Co) phase during thermal crystallization, so that the grain size does not increase with increasing holding time.  $H_c$  increases for the longer holding time. The increase of  $H_c$  is due to the increase of grain size and the precipitation of  $Fe_3Zr(B)$  phase which has larger magnetocrystalline anisotropy.<sup>20</sup>

Annealing of the RQ alloy leads to the disappearance of the H-phase and spontaneous vitrification occurs by the solid state reaction. The transformation also depends on cooling rate after annealing. TEM images, the corresponding

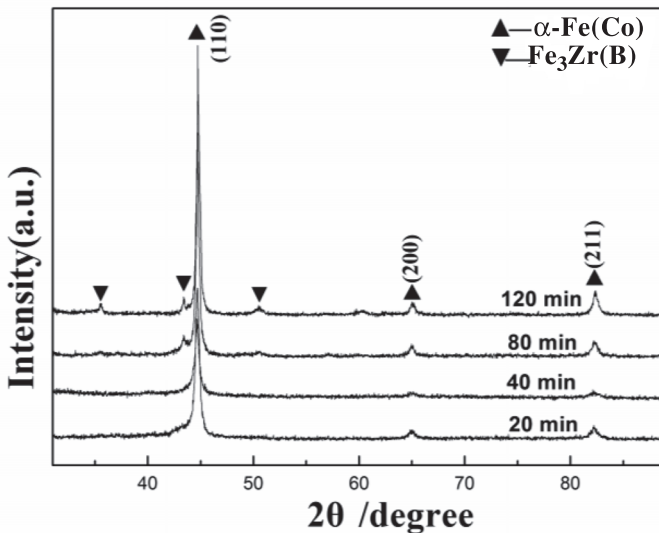


Fig. 5. XRD patterns of Fe<sub>77</sub>Co<sub>2</sub>Zr<sub>9</sub>B<sub>10</sub>Cu<sub>2</sub> alloys annealed at 600°C for different holding times.

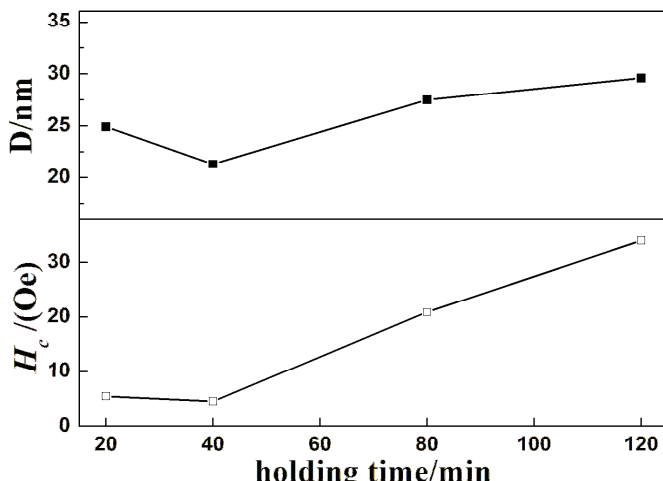


Fig. 6. Grain size ( $D$ ) of  $\alpha$ -Fe(Co) and coercivity ( $H_c$ ) as a function of holding time.

selected area diffraction patterns (SADP) and grain size distribution profiles of Fe<sub>77</sub>Co<sub>2</sub>Zr<sub>9</sub>B<sub>10</sub>Cu<sub>2</sub> alloys annealed at 600°C followed by furnace cooling #1 (a, a') and liquid-nitrogen cooling #2 (b, b') are shown in Fig. 7. Figure 7(a) shows that the crystalline phase of sample #1 consists of the  $\alpha$ -Fe(Co) grains. The mean grain size from grain size distribution profile is about 15.2 nm, which is smaller than that was calculated by Scherer's formula in Fig. 6 (21.3 nm). It should be noted that

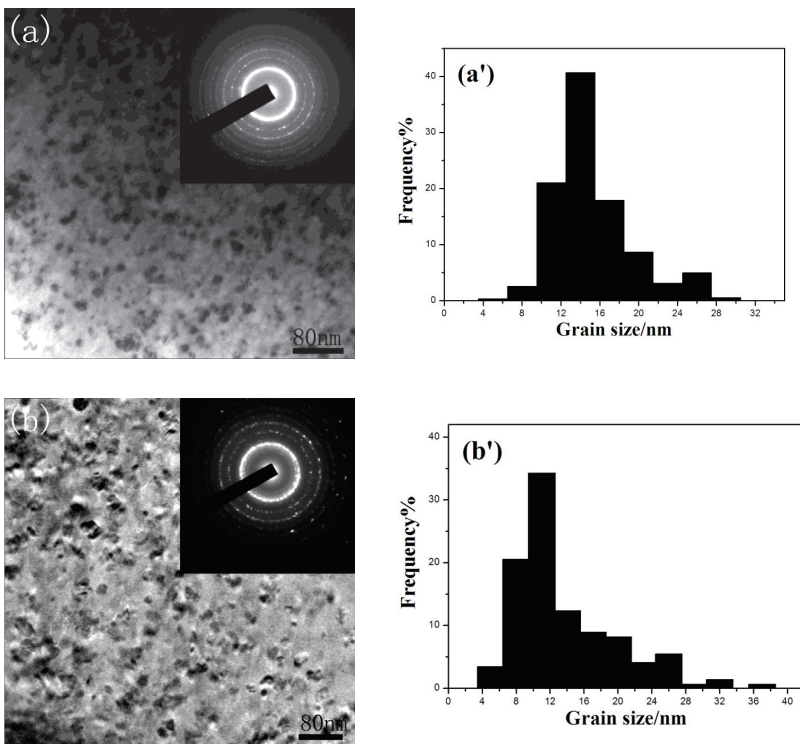


Fig. 7. TEM images, the corresponding selected area diffraction patterns (SADP) and grain size distribution profiles of  $Fe_{77}Co_2Zr_9B_{10}Cu_2$  alloys annealed at  $600^{\circ}C$  followed by furnace cooling (a, a') and liquid-nitrogen cooling (b, b').

some of the large grain formed during heat treatment were detected by XRD, but not found and not counted in the grain size distribution profiles from TEM. There is a little residual H-phase observed except for  $\alpha$ -Fe(Co) phase in the Fig. 7(b). The rapid quenching in liquid-nitrogen results in that H-phase does not transform into  $\alpha$ -Fe(Co) phase completely. The mean grain size is about 13.8 nm. The corresponding  $H_c$  of two alloys are 4.5 Oe and 16.4 Oe, respectively.  $H_c$  of sample #2 is higher, which is due to the stress caused by rapid quenching in liquid-nitrogen and the existence of residual H-phase.

#### 4. Conclusion

(i)  $Fe_{77}Co_2Zr_9B_{10}Cu_2$  alloy as-quenched is a mixture of  $\alpha$ -Fe(Co) phase, H-phase and amorphous phase. The content of H-phase in the free surface is higher than that in the contact surface, and the corresponding amorphous phase in the free surface is lower than that in the contact surface. Microstructures between free and contact surface after heat treatment have little difference. H-phase is metastable and transforms to  $\alpha$ -Fe(Co) phase during thermal crystallization.

W. Q. Yu et al.

(ii) The three exothermal peaks in the DTA curve correspond to the transformation of H-phase, the crystallization of residual amorphous phase and the precipitations of  $\text{Fe}_3\text{Zr}(\text{B})$  intermetallic compounds, respectively.

(iii)  $\text{Fe}_{77}\text{Co}_2\text{Zr}_9\text{B}_{10}\text{Cu}_2$  alloy as-quenched is annealed at different heat treatment conditions. Annealing of the RQ alloy leads to the disappearance of the H-phase and the transformation also depends on cooling rate after annealing. Coercivity ( $H_c$ ) of  $\text{Fe}_{77}\text{Co}_2\text{Zr}_9\text{B}_{10}\text{Cu}_2$  alloy annealed at  $600^\circ\text{C}$  for 40 min followed by furnace cooling has the minimum value, which is attributed to the small and homogeneous  $\alpha$ -Fe(Co) grain structure.  $\text{Fe}_{77}\text{Co}_2\text{Zr}_9\text{B}_{10}\text{Cu}_2$  alloys annealed at  $600^\circ\text{C}$  followed by liquid-nitrogen cooling has smaller grain size and a small amount of H-phase. However, due to the stress caused by rapid quenching in liquid-nitrogen and the existence of residual H-phase, it has higher coercivity.

### Acknowledgments

This work was funded by Science and Technology Development Project of Jilin Province (No. 201105083), Science and Technology Studying Project of “12th five-year” Office of Education of Jilin Province (No. 2014-485) and Graduate Innovative Research Programs of Jilin Normal University (No. 201103).

### References

1. Z. Hua, Y. M. Sun, W. Q. Yu and M. B. Wei, *Int. J. Mod. Phys. B* **26** (2012) 1250088-1.
2. A. Makino, T. Bitoh, A. Inoue and T. Masumoto, *J. Appl. Phys.* **81** (1997) 2736.
3. T. Nagase and Y. Umakoshi, *ISIJ Int.* **46** (2006) 1371.
4. A. Fernández-Martínez, P. Gorría, G. J. Cuello, J. D. Santos and M. J. Pérez, *J. Non-Cryst. Solids* **353** (2007) 855.
5. S. Stankov, B. Sepiol, T. Kauch, D. Scherjau, R. Würschum and M. Miglierini, *J. Phys.: Condens. Matter* **17** (2005) 3183.
6. J. C. Tang, A. H. Wu, X. Y. Mao, S. D. Li, W. L. Gao and Y. W. Du, *J. Phys. D: Appl. Phys.* **37** (2004) 151.
7. W. S. D. Folly, V. R. Caffarena, R. L. Sommer, J. L. Capitaneo and A. P. Guimarães, *J. Magn. Magn. Mater.* **320** (2008) 358.
8. Y. M. Sun, W. Q. Yu and Z. Hua, *Acta Phys. Pol. A* **119** (2011) 374.
9. K. Suzuki, G. Herzer and J. M. Cadogan, *J. Magn. Magn. Mater.* **177–181** (1998) 949.
10. K. Suzuki and J. M. Cadogan, *J. Appl. Phys.* **85** (1999) 4400.
11. Y. X. Wang, Y. Ju, W. Lu, B. Yan and W. Gao, *Mod. Phys. Lett. B* **27** (2013) 1341024.
12. K. Suzuki, J. M. Cadogan, V. Sahajwalla, A. Inoue and T. Masumoto, *J. Appl. Phys.* **79** (1996) 5149.
13. J. C. Tang, X. Y. Mao, S. D. Li, W. L. Gao and Y. W. Du, *J. Alloys Compd.* **375** (2004) 233.
14. I. V. Lyasotskii, N. B. Dyakonova, E. N. Vlasova, D. L. Dyakonov and M. Yu. Yazvitskii, *Phys. Status Solidi A* **203** (2006) 259.
15. I. V. Lyasotsky, N. B. Dyakonova, D. L. Dyakonov, E. N. Vlasov and M. Y. Jazvitsky, *Rev. Adv. Mater. Sci.* **18** (2008) 695.

16. W. Q. Yu, Y. M. Sun, Y. D. Liu, J. Liu, B. Zuo, L. H. Liu, L. R. Dong and Z. Hua, *Optoelectron. Adv. Mater. Rapid Commun.* **6** (2012) 145.
17. A. Takeuchi and A. Inoue, *Mater. Trans.* **46** (2005) 2817.
18. H. Huang, G. Shao and P. Tsakirooulos, *J. Alloys Compd.* **459** (2008) 185.
19. V. Andronis and G. Zografi, *J. Non-Cryst. Solids* **271** (2000) 236.
20. B. Li, X. J. Yu, W. Han and K. An, *Mater. Trans.* **48** (2007) 6.